HHS Public Access

Author manuscript

J Control Release. Author manuscript; available in PMC 2021 November 10.

Published in final edited form as:

J Control Release. 2020 November 10; 327: 174–185. doi:10.1016/j.jconrel.2020.07.040.

Towards "CO in a pill": Pharmacokinetic studies of carbon monoxide prodrugs in mice

Minjia Wang[a], **Xiaoxiao Yang**[b], **Zhixiang Pan**[b], **Yingzhe Wang**[a], **Ladie Kimberly De La Cruz**[b], **Binghe Wang**[b,*], **Chalet Tan**[a,*]

[a]Department of Pharmaceutics and Drug Delivery, University of Mississippi School of Pharmacy, University of Mississippi, MS 38677, USA

[b]Department of Chemistry and Center for Diagnostics and Therapeutics, Georgia State University, Atlanta, GA 30303, USA

Abstract

Carbon monoxide (CO) is a known endogenous signaling molecule with potential therapeutic indications in treating inflammation, cancer, neuroprotection, and sickle cell disease among many others. One of the hurdles in using CO as a therapeutic agent is the development of pharmaceutically acceptable delivery forms for various indications. Along this line, we have developed organic CO prodrugs that allow for packing this gaseous molecule into a dosage form for the goal of "carbon monoxide in a pill." This should enable non-inhalation administration including oral and intravenous routes. These prodrugs have previously demonstrated efficacy in multiple animal models. To further understand the CO delivery efficiency of these prodrugs in relation to their efficacy, we undertook the first pharmacokinetic studies on these prodrugs. In doing so, we selected five representative prodrugs with different CO release kinetics and examined their pharmacokinetics after administration *via* oral, intraperitoneal, and intravenous routes. It was found that all three routes were able to elevate systemic CO level with delivery efficiency in the order of intravenous, oral, and intraperitoneal routes. CO prodrugs and their CO-released products were readily cleared from the circulation. CO prodrugs demonstrate promising pharmaceutical properties in terms of oral CO delivery and minimal drug accumulation in the body. This represents the very first study of the interplay among CO release kinetics, CO prodrug clearance, route of administration, and CO delivery efficiency.

Keywords

Carbon monoxide (CO); Organic CO prodrugs; Pharmacokinetics; Carboxyhemoglobin (COHb); Fecal analysis; Controlled release

*Corresponding authors. wang@gsu.edu (B. Wang), chalettan@olemiss.edu (C. Tan).

Credit author statement

M.W. designed and performed all *in vitro* and *in vivo* experiments. Y.W. contributed to the pharmacokinetic analysis. X.Y., Z.P., L.K.D.L.C. and B.W. were responsible for the chemistry support, analysis of how pharmacokinetic studies affect the utility of CO prodrugs, and selection of prodrugs to study. B.W. and C.T. conceived the project and supervised all experiments. M.W., X.Y., B.W. and C.T. wrote the manuscript with all authors participating in the discussion and revision.

Appendix A. Supplementary data

Supplementary data to this article can be found online at https://doi.org/10.1016/j.jconrel.2020.07.040.

1. Introduction

Carbon monoxide (CO) is widely known as a poisonous gas. Less known is its role as a signaling molecule with therapeutic effects [1–5]. CO is endogenously produced in mammals through heme degradation by heme oxygenase (HO). In human, CO production is an ongoing process as part of red blood cell turnover, leading to the generation of about 400 μmol of CO every day. CO is largely stored in the form of CO-bound hemoglobin, carboxyhemoglobin (COHb) [3]. Recent years have seen a surge of interest in CO [2,6–9] because of its demonstrated therapeutic effect in treating conditions such as inflammation [10], drug-induced toxicity [11,12], ischemia reperfusion injury [13] among others. In developing CO-based therapeutic agents, one key issue is the availability of pharmaceutically acceptable ways of delivering CO. During the past decade, there has been a large number of experiments in cell culture, animal models, and clinical trials using CO gas [2,14]. These experiments have contributed enormously to the understanding of CO physiology and pharmacology. However, it is hard to control dosage and CO poisoning is a serious risk when CO gas is used. For controlled CO dosage and minimized safety risk, liquid and solid formulations are preferred under most circumstances. Along this line, CO in a liquid formulation [15], immobilized carbonyls [16], and organic CO donors have been developed [6,9,17–22]. The very first biological experiment using immobilized carbonyls to assess CO's biological activity was conducted in 1891 by McKendrick and Snodgrass using nickel tetracarbonyl [23]. Later on, the Motterlini lab initially experimented with known metal-immobilized CO molecules as CO-releasing molecules (CO-RMs) for therapeutic applications [24]. Aimed at improving various delivery properties, Motterlini and Mann, Mascharak, Schiller, Schmalz, Boyer and others developed some of the later versions of CO-RMs including enzyme-activated forms [2,25–30]. There have also been efforts in encapsulating metal-based CO-RMs for reduced metal exposure [31–33]. The Motterlini lab has recently reported hybrid CO-RMs through conjugation with an activator of HO-1 with the aim of creating synergy with endogenously produced CO [34,35]. These metal-immobilized carbonyls have played a very significant role in understanding CO physiology and in demonstrating pharmacological efficacy in various animal models. However, in recent years, there have been discussions of what roles that transition metal plays in some of the observed biological effects with important questions raised as to whether the observed effects can be solely attributed to CO; how much CO is released under physiological conditions, the ability for the CO-RMs to react with proteins and undergo/facilitate other reactions; and the cytotoxicity and other biological effects of the metal component [7,26–28,36–38]. A recent study also showed that the widely reported effect of ruthenium-based CO-RMs (CORM-2, -3) on coagulation [39] is *via* a CO-independent mechanism, suggesting the importance of looking at the metal carrier in examining the effects of CO-RMs [40]. As further examples of issues that need to be addressed, ruthenium-based CORM-3 can undergo water-shift reaction to release H_2 and CO_2, can release CO with widely variable rates depending on the conditions and other species present, and may sequester NO [25,26]. It was also suggested that other iron- or manganese-based CO-RMs might catalyze the Fenton reaction [25]. In a very recent study, it was shown that CORM-2,3 are active as reducing agents with the ability to reduce arylnitro groups [41]. Therefore, there have been very active efforts in search of alternatives that do not rely on CO

immobilized on a metal center. For example, Berreau, Popik, Liao, and Klan have worked on photo-sensitive organic CO-RMs [6,8,9,17–20,42]. There are also others who used biologically compatible hemoglobin as a "carrier" for CO [43,44]. However, regardless of whether there is metal involved, one would have to be concerned about the effect of the "carrier" molecules, including some of the newer organic CO donors developed in our own lab that are metal-free [1,4,6]. Therefore, careful controls are needed. Collectively, all the issues discussed this far bring to the forefront of the subject of "developability" or "drug-like" properties. This would require us to think beyond the issue of whether a donor molecule would "*release*" CO and shift the focus to its likelihood of serving the role of a prodrug with desirable pharmaceutical properties, including issues of toxicity, chemical tractability, delivery properties, unintended reactions, among others.

Generally speaking, there are two approaches to address this issue: (1) finding ways to minimize systemic exposure of the "carrier" molecule and (2) using "carrier" molecules that have minimal or manageable safety-related problems and have no or minimal "off-target" chemical and biological activities. Along this line, there have been some very clever approaches developed in minimizing the systemic exposure of transition metal ions from metal-based CO-RMs [16,32,45]. We are very interested in developing metal-free organic prodrugs of CO for therapeutic applications. By taking advantage of a Diels-Alder reaction, we have developed bimolecular [11,46] and unimolecular CO prodrugs [4,47] with tunable release rates, triggered release by pH, esterase, and ROS [10,47–49], targeted release [11], and the ability to carry two payloads in one molecule [50–52]. The Larsen lab has also reported a class of organic CO prodrugs, which are pH-sensitive [53]. The structural diversity of these CO prodrugs allows for much medicinal chemistry effort to suit the need of various applications with the eventual goal of being able to pack "carbon monoxide in a pill". One can also envision various routes of administration of these prodrugs in animal model studies and possibly in humans at a later stage. One of the questions in the CO field is the lack of understanding of the pharmacokinetic properties of various CO donors, especially with the organic CO prodrugs. This is a complex issue and may very well be species-dependent. As a first step, we examined organic CO prodrugs with different CO release half-lives with the following questions in mind: (1) can orally delivered CO prodrugs lead to elevated levels of CO using COHb as an indicator; (2) how different delivery routes (*i.v.*, *i.p.*, and *p.o.*) compare in terms of the efficiency in systemically delivering CO as measured by COHb levels; (3) whether CO released inside the gastrointestinal tract is systemically available; and (4) to what degree we can minimize systemic exposure of the "carrier" molecule. In doing so, we selected five CO prodrugs (Fig. 1) including CO-103, CO-104, CO-115, CO-116, and CO-125 with varying CO release half-lives, as reported earlier when studied in a mixture of PBS and DMSO [4,54]. The corresponding CO-released products (CP products) CP-103, CP-104, CP-125, CP-115, and CP-116 (Fig. 1) were synthesized to allow for direct quantification of the CP products of the CO prodrugs *in vitro* and *in vivo*. Previous biological studies have demonstrated that these organic CO prodrugs at low micromolar range potently attenuated lipopolysaccharide-induced inflammatory response in RAW264.7 cells while the prodrugs themselves and their corresponding CP products caused minimal cytotoxicity [4]. Importantly, the therapeutic efficacy of several organic prodrugs has been demonstrated in murine models of chemically induced colitis [4],

systemic inflammation and associated liver injury [10], kidney reperfusion injury [13], chemically induced gastric injury [55], and chemically induced liver injury [11]. Herein we report the results of detailed pharmacokinetic studies on these five metal-free CO prodrugs in mice at dose levels comparable to those that have allowed us to observe efficacy in animal models.

2. Experimental methods

2.1. Ethics statement

CD-1 mice (25–30 g) were purchased from Envigo (Indianapolis, IN, USA). Equal numbers of male and female mice were used in each experiment. All animal procedures were conducted in accordance with the Guide for the Care and Use of Laboratory Animals of the National Institute of Health. The animal procedure protocols were approved by the Institutional Animal Care and Use Committee at the University of Mississippi (IACUC protocol number: 19–012).

2.2. Chemicals and reagents

CO prodrugs including CO-103, CO-104, CO-125, CO-115, and CO-116 and their corresponding CO-released products CP-103, CP-104, CP-125, CP-115, and CP-116 were synthesized as described previously [4,54]. Stocks and working solutions of CO prodrugs and CP products were prepared in dimethyl sulfoxide (DMSO) and stored at −80 °C. Kolliphor® HS 15 (Kolliphor) was from BASF (New York, NY, USA). Simulated gastric fluid (SGF, 0.2% (*w*/*v*) sodium chloride in 0.7% (*v*/v) hydrochloric acid, pH 1.0–1.4) and simulated intestinal fluid (SIF, without pancreatin, USP XXII formulation, containing potassium dihydrogen phosphate and sodium hydroxide, pH 7.4–7.6) were obtained from Ricca Chemical (Arlington, TX, USA). Deionized water from a Milli-Q-UF system (Millipore, Milford, MA, USA) was used. All other chemicals were of analytical grade.

2.3. Sample extraction

The plasma or liver homogenate samples were extracted by a salting-out assisted liquid/liquid extraction method [56–58] and maintained at 4 °C throughout the process. For a 20 μl plasma sample, 1 μl of α-naphthoflavone (α-NF, 200 μM) was spiked in as an internal standard. Then 20 μl of sodium chloride (4 M) and 80 μl of acetonitrile were added and mixed. Phase separation occurred as a result of the salting-out effect. After vigorous vortexing and centrifugation at 10,000*g* for 5 min, 75 μl of the upper layer was aspirated, mixed with 40 μl of phosphate buffer (pH 3) and directly injected into the HPLC. A similar extraction method was developed for the liver homogenate samples.

2.4. Analytical methods

The Agilent 1260 Infinity II HPLC system (Agilent Technologies, Palo Alto, CA) equipped with an autosampler, a PDA detector, and an OpenLAB CDS computer system was used to quantify the concentration of CO prodrugs and CP products. An Agilent Poroshell 120 EC-C18 column (2.7 μm, 3 × 150 mm) with a guard column (3.5 μm, 3 × 3 mm) was used. A gradient elution method was applied to all the CO prodrug/CP product pairs. The calibration curves for all CO prodrugs and CP products were established. α-NF was used as an internal

standard for all CO/CP compounds. The HPLC conditions were summarized in the Supplementary Information (Section I, Table S1). The HPLC methods for analyzing the concentration of the CO prodrug/CP product pairs in plasma, liver homogenate and fecal samples were developed separately and validated with respect to selectivity, linearity, sensitivity, extraction recovery, stability, precision, and accuracy (Supplementary Information Section II). The COHb level in the whole blood was measured using a CO-oximeter (AVOXimeter 4000, Avox Systems, New York, NY, USA). The CO-oximetry measurement strictly followed the manufacturer's protocol and was also validated for accuracy and precision by performing quality control protocols using both optical controls and liquid controls on a daily basis.

2.5. In vitro transformation studies

The CO prodrugs were incubated in simulated intestinal fluid (SIF), simulated gastric fluid (SGF), plasma, liver homogenate, or albumin solution at 37 °C. The final content of DMSO was 50% (v/v) in SIF or SGF, 1% (v/v) in plasma, liver homogenate, or albumin solution; the final content of Kolliphor was 2% (w/v) in SIF or SGF. The samples were collected at pre-determined time points and analyzed for the concentrations of the CO prodrugs and CP products by HPLC. To derive the first-order rate constant (k) for the conversion reaction from each CO prodrug to the corresponding CP product, the CO prodrug concentration (C_t) as a function of incubation time (t) was fitted to the equation $C_t/C_o = e^{-kt}$, wherein C_o is the initial prodrug concentration at time zero. The best-fit nonlinear regression was obtained by GraphPad Prism (San Diego, CA, USA).

2.6. Plasma protein binding

An ultrafiltration method was used to determine the plasma protein binding of the compounds [59,60]. Briefly, CO prodrugs (1 mM) in DMSO were spiked into 200 μl of mouse plasma at a ratio of 1:100 to give a final concentration of 10 μM. α-NF was used as the internal standard. The spiked plasma was vigorously vortexed and equilibrated at 37 °C for 5 min. Samples were then transferred to a Microcon centrifugal filter unit with a molecular-weight cutoff (MWCO) of 30 kDa (Microcon YM-30, Millipore, Bedford, MA, USA), and centrifuged (10,000*g*, 4 °C, 10 min). This size-exclusion method allows for the protein-bound prodrug to remain in the top compartment and the unbound to filter through into the bottom compartment. The CO prodrug concentration in the top plasma concentrate and the bottom filtrate solution were analyzed by HPLC as described above, and the volume of each fraction was measured. All experiments were performed independently at least three times, each with triplicate samples.

2.7. Pharmacokinetic studies

CO prodrugs or CP products were dissolved in Kolliphor/PBS (1:2 *v*/v or 1:3 *v*/v) at a stock concentration of 5 mg/ml, which was confirmed by HPLC. The drug-loaded formulation or the blank vehicle was administered in fed mice ($n \geq 3$) *via* oral gavage (*p.o.*) administration, intraperitoneal (*i.p.*), or intravenous (*i.v.*) injection. At pre-determined time points post administration, blood samples were collected by retro-orbital bleeding and kept on ice to prevent CO prodrugs from undergoing the CO-release reaction. Fecal samples were also collected. Circulating CO was monitored by measuring the COHb level in the whole blood

using a CO-oximeter (AVOXimeter 4000, Avox Systems, New York, NY, USA). The baseline COHb level of each mouse was measured before administration. The plasma concentrations of each CO prodrug and the corresponding CP product were simultaneously quantified by HPLC. Non-compartmental analysis was performed by using WinNonlin® version 6 (Pharsight, MountainView, CA, USA) to obtain the pharmacokinetic parameters of the CO prodrugs and CP products, including the terminal half-life ($t_{1/2}$), area under the curve ($AUC_{0-\infty}$), total body clearance (CL_T), and bioavailability (F). The area under the COHb level curve (COHb AUC) was estimated using GraphPad Prism (San Diego, CA, USA).

2.8. Fecal analysis

Following oral administration of CO-103 or CP-103 in mice, feces were collected every 2 h, weighed into Eppendorf tubes, and stored at −20 °C. To extract CO-103 and CP-103, the fecal samples were kept at 4 °C throughout the extraction process. The fecal samples (50–80 mg per aliquot) were spiked with α-NF as internal standard, soaked in NaCl solution (4 M, 400 μl), and then homogenized using grinder, vortex mixer, and bath sonication. The homogenized fecal samples were extracted by acetonitrile (800 μl) with vigorous vortexing for 30 min. The samples were then centrifuged at 10,000 rpm for 5 min; the supernatants (2 μl) were mixed with 22 μl of the mobile phase [70% acetonitrile and 30% phosphate buffer (pH 3)] for HPLC analysis.

2.9. Statistical analysis

All data were presented as the mean ± standard deviation ($n \geq 3$). Statistical analysis was performed by Student's *t-test* for comparison between two groups, and one-way ANOVA followed by Bonferroni post-hoc analysis for comparison among three or more groups using SPSS v24.0 (SPSS Inc., Chicago, IL, USA). A p-value of less than 0.05 (*) was considered to be statistically significant.

3. Results and discussion

3.1. Establishment of simultaneous quantification for CO prodrug/CP product pairs by HPLC

As the first step, we established highly sensitive and reproducible HPLC methods to quantify each CO prodrug and its corresponding CP product simultaneously in aqueous buffers, plasma, liver homogenate, and fecal samples. The selectivity of the methods is shown in the representative chromatograms of CO/CP pairs in plasma (Supplementary Figs. S1–S5) and feces (Supplementary Fig. S6). A rapid salting-out assisted liquid/liquid extraction method yielded a recovery rate of ≥70% for all tested CO prodrugs and CP products in plasma, liver homogenate, and fecal samples. With reversed-phase HPLC, given the well-resolved chromatograms and strong signal responses, we were able to achieve a quantification limit of 0.1 μM per 20 μl biological matrices for CO-103/CP-103, CO-104/CP-104, CO-125/CP-125, CO-115/CP-115, and CO-116/CP-116 pairs. The linear ranges for the quantification of the CO prodrugs and CP products were the same, between 0.1 and 20 μM. All tested CO prodrugs and CP products remained intact in the biological samples for at least 6 h at 4 °C and 24 h at −18 °C, as indicated by the recovery of over 95% of the

respective compounds from these matrices. The detailed validation information is provided in the Supplementary Information (Section II).

3.2. Stoichiometric conversion of CO prodrugs to CP products in biological buffers and matrices

Although the CO prodrugs studied here have been tested in our previous studies showing the stoichiometric and tunable CO release in PBS/DMSO mixture [4,54], we were interested in broadening such studies to include SIF, SGF, plasma, and liver homogenates in order to gain a fuller understanding of the effects of various factors on the CO release rates. The low aqueous solubility of the CO prodrugs necessitated the inclusion of an organic solvent such as DMSO or a solubilizer such as Kolliphor when constituting aqueous solutions of these compounds. We chose to include 50% (*v*/v) DMSO or 2% (*w*/*v*) Kolliphor to ensure the complete solubilization of all tested CO prodrugs in aqueous buffers. *In vitro* incubation studies were first performed in SIF that mimics the neutral aqueous milieu in the small intestines with a final DMSO concentration of 50% (v/v). As expected, the CO prodrugs readily underwent conversion to CP products in the aqueous environment, and the decline in the CO prodrug levels clearly followed first-order reaction kinetics (Fig. 2), from which the CO release half-life was estimated for each CO prodrug (Table 1). While the reaction kinetics of CO-115 and CO-116 was unaffected in the presence of DMSO or Kolliphor, CO releases from CO-103, CO-104 and CO-125 were markedly prolonged in SIF (2% Kolliphor) ($p < 0.05$). This is likely owing to the retention of these CO prodrugs within micelles formed by Kolliphor (Supplementary Fig. S7), resulting in hampered reaction kinetics. This could explain the drastic prolongation of the reaction half-life of CO-104 in SIF (2% Kolliphor), which had the highest lipophilicity among the five CO prodrugs (Supplementary Fig. S8). Being less lipophilic with the presence of a morpholine group, CO-115 and CO-116 may readily diffuse from Kolliphor micelles into the aqueous solution, and their reaction rates were thus not influenced by the physical entrapment. Therefore, the reaction kinetics observed in Kolliphor-containing buffers may not necessarily reflect the true reactivity of all CO prodrugs. On the other hand, the Diels-Alder reaction needed for CO release is known to be accelerated by water and impeded by organic solvents such as DMSO [6,61,62]. As a result, the CO-103 reaction kinetics was notably more rapid in SIF with 50% DMSO than that in 80–100% DMSO (Supplementary Fig. S9). However, the fact that the conversion reaction occurred at a similar rate in SIF with 20% or 50% DMSO (Supplementary Fig. S9) suggests that once the DMSO solution is sufficiently diluted by the aqueous solution, the accelerating effect of increased water content on the Diels-Alder reaction becomes diminished. Similar findings were observed with the other four CO prodrugs. Therefore, the reaction rates of CO prodrugs measured in SIF with 50% DMSO may represent a reasonable approximation of the chemical conversion kinetics in SIF. Among all tested CO prodrugs, CO-103 exhibited the most rapid reaction kinetics while CO-115 being the slowest. These findings are in accordance with previous reports [4,54].

Interestingly, the conversion reactions of CO-103, CO-104, and CO-125 were somewhat retarded in plasma, as indicated by the prolonged reaction half-lives compared to those in SIF (50% DMSO) ($p < 0.05$). It is likely that plasma protein binding imposes conformational constraints to impede the intramolecular Diels-Alder reaction and thus slows

down the conversion to the CP products and CO release. Indeed, CO-103, CO-104, and CO-125 were found to be highly protein-bound (92%, 91%, and 90%, respectively) in plasma, whereas the plasma protein binding of CO-115 and CO-116 was less extensive (84% for both). Not only the extent of plasma protein binding, but also the site of binding may cause different hindrance. In addition, the conversion of CO-103 in an albumin solution (50 mg/ml in PBS) had similar half-life as in plasma (1.58 h *vs* 1.29 h), suggesting albumin as the primary protein component accounting for plasma protein binding (Supplementary Fig. S10). It is worth mentioning that because of the high degree of plasma protein binding, all tested CO prodrugs could be completely solubilized in plasma at up to 50 μM with minimal addition of DMSO (< 0.5%).

The CO prodrugs were found to undergo spontaneous and stoichiometric conversion to the CP products in plasma and SIF (50% DMSO) (Fig. 3 and Supplementary Fig. S11). In addition to SIF, identical kinetic profiles were obtained in SGF (50% DMSO) that simulates the acidic gastric fluid (Supplementary Fig. S12), indicating that the conversion reaction of these CO prodrugs is pH-independent. Surprisingly, all five CO prodrugs reacted at a slower rate in the liver homogenate than in SIF (Supplementary Fig. S12), arguing against the involvement of hepatic enzymes in the conversion reaction as one would have expected. As the CO prodrugs reacted in the liver homogenate, stoichiometric amounts of the CP products were recovered without the detection of alternative degradation products. Further, all five CP products were stable in the liver homogenate and plasma, indicating that the CP compounds are not prone to enzymatic metabolism in the liver or plasma.

3.3. Systemic CO delivery and biodisposition of the CO prodrugs in mice

Kolliphor® HS 15, an FDA-approved amphiphilic excipient, was selected as the solubilizing agent for CO prodrugs and CP products. It was found that the solubility for each tested compound was at least 10 mg/ml. Importantly, unlike common organic solvents such as DMSO and ethanol, Kolliphor did not cause hemolysis or disturb the COHb baseline when administered *i.v.* (< 10 μl), *p.o.* (< 50 μl) or *i.p.* (< 30 μl). Pharmacokinetics of CO-103 was investigated in detail following *p.o.*, *i.p.* and *i.v.* administration in mice. CO released from the prodrug, as measured by the COHb level in whole blood, is a critical endpoint that correlates with how effective the CO prodrug may systemically deliver CO *in vivo*. The baseline level of COHb in healthy mice usually ranged between 0.3 and 1.5%. As shown in Fig. 4A, the COHb level rose quickly following *p.o.* administration of CO-103 (25 mg/kg) with t_{max} of around 1 h and remained elevated above the baseline for 1.5 h ($p < 0.05$). The COHb level did not rise above the baseline following *p.o.* administration of pure CP-103 or blank vehicle, indicating the elevated COHb level was the net result of the prodrug only. In contrast, *i.p.* injection of CO-103 at the same dose only caused an increase in COHb level at 0.5 h (Fig. 4B). Elevated COHb level for a longer duration was observed after *i.v.* injection of CO-103 at a much lower dose (5 mg/kg) as compared to *p.o.* and *i.p.* administration (Fig. 4C). CO exposure in the circulation, reflected by COHb *AUC*, which is defined as the area under the blood COHb level subtracting the pre-administration baseline from time zero to the last sampling time point, was used to estimate the systemically absorbed CO. CO delivery efficiency is defined as the percentage of COHb *AUC* in relation to that of *i.v.* administration at an equivalent dose. As shown in Table 2, *p.o.* administration of CO-103

achieved systemic CO delivery with a relative efficiency of 11.7%, compared to that of *i.v.* injection, whereas significantly lower efficiency (3.7%) was observed with *i.p.* dosing.

To investigate the absorption as well as the transformation of CO-103 to CP-103, the plasma levels of CO-103 and CP-103 were assessed following the administration of CO-103 (Fig. 4A-C). As expected, the bioavailability of CO-103 following *p.o.* administration was significantly lower than *i.p.* administration (9.2% *vs.* 33.8%) (Table 2). However, it is intriguing to observe that *p.o.* administration appears to be more effective in delivering CO systemically (Fig. 4A and B). With significantly more CO-103 being available in the circulation (indicated by $AUC_{0-\infty}$ of CO-103, $p < 0.05$) but lower CO exposure (indicated by COHb *AUC*, $p < 0.05$) following *i.p.* than *p.o.* administration (Table 2), such results support the idea that the release of CO from CO-103 occurs more readily and extensively in the gastrointestinal tract than within the intraperitoneal cavity. These results also support the notion that CO generated in the gastrointestinal tract is readily absorbed into the systemic circulation, as one would expect based on other studies [15,63]. Estimated by comparing the plasma profiles of *i.v.* and *p.o.* administered CP-103 (Fig. 4D and E), the oral bioavailability of CP-103 was 29.2%. The key pharmacokinetic parameters for CO-103 and CP-103 are summarized in Table 2. It is worth mentioning that the terminal half-life of pure CP-103 was shorter ($p < 0.05$) than that of CP-103 generated *in situ* through the administration of CO-103 for all delivery routes. This may be rationalized that the half-life of CP-103 may be dominated by its formation from CO-103 *in vivo*. CO-103 *p.o.* administration only led to 9% bioavailability compared with *i.v.* administration. Interestingly, the three administration routes examined herein all gave a similar COHb peak level about 3–4% despite the differences in the CO release half-life, time to peak, peak duration (Fig. 4), and bioavailability (Table 2). The therapeutic efficacy of CO-103 has been previously evaluated in a murine colitis model. Following multiple *i.p.* doses at 15 mg/kg, CO-103 markedly improved colon length, thickness, and injury scores, resulting in an increased survival rate [4]. From the pharmacokinetic findings described above, it is reasonable to conclude that CO exposure resulting from *p.o.* and *i.p.* administration of CO-103 is therapeutically relevant. In particular, these results demonstrate the promise of CO-103 for oral CO delivery.

Next, we evaluated the pharmacokinetics of CO-104, a close analog of CO-103 that showed 10-fold slower reaction kinetics in SIF (Table 1). Interestingly, *p.o.* and *i.p.* administration of CO-104 (25 mg/kg) only caused a modest (below 3%) and brief increase in the COHb level (Fig. 5) compared to CO-103, indicating limited CO production *in vivo*. While the resulting plasma concentration of the prodrug CO-104 was notably higher than CO-103, the level of the released product CP-104 was rather subdued following *p.o.* administration and was undetectable in *i.p.*-dosed mice. This suggests that even though CO-104 is absorbed from the gastrointestinal tract or the abdominal cavity, its conversion to CP-104 in the circulation occurs to a rather limited degree before CO-104 is cleared from the bloodstream or is metabolized to a different product. These findings highlight the importance of optimizing the reaction kinetics, because CO prodrugs with a long release half-life may get eliminated prior to the significant CO release *in vivo*.

Following the *p.o.* dosing of CO-125 at 25 mg/kg, the COHb level peaked at around 3% at 1 h and returned to the baseline at 4 h. While the plasma level of CO-125 was below the

quantification limit, CP-125 gradually increased to 0.4 μM and peaked at 1.5 h (Fig. 6A). Considering the rapid conversion from CO-125 to CP-125 in aqueous fluids ($t_{1/2} < 1$ h), the lack of a detectable level of CO-125 suggests that the release of CO takes place mostly in the GI tract with minimal absorption of CO-125 into the circulation. To assess the extent of formation and systemic absorption of CP-125 resulted from CO-125 *p.o.* dosing, the plasma CP-125 level *vs.* time curve (Fig. 6A) was compared with that following *i.v.* and *p.o.* administration of pure CP-125 (Fig. 6B and C). The oral bioavailability of CP-125 was found to be 6% (Table 3). It is important to note that the values of $t_{1/2}$ and $AUC_{0-\infty}$ were nearly identical for CO-125-derived CP-125 and pure CP-125. Such results strongly suggest that CO-125 is completely converted to CP-125 in the gastrointestinal tract and the released CO gets absorbed into the circulation, leading to an elevated COHb level. It is important to note that CO/CP-125 contain a morpholine moiety, which is designed to improve water solubility and attenuate membrane permeability. This is because the free morpholine amine group is expected to largely remain in the protonated form under physiological conditions, leading to increased hydrophilicity and decreased passive membrane permeability. The low systemic bioavailability of CO-125 and CP-125 is desirable and minimizes the systemic exposure of components other than CO.

Lastly, following CO-115 and CO-116 *p.o.* administration, the COHb level also rose readily to 3–4% and both peaked at around 1 h, and plasma levels of CP-115 and CP-116 reached C_{max} at around 0.5–1 h (Fig. 7). CO-115 and CO-116 share a common scaffold except for the methyl substitution in the “linker” portion in CO-116 that is known to impose conformational constraints and thus imparts higher cycloaddition reactivity [54]. The fast-release prodrug CO-116 was found to result in much higher COHb *AUC* as compared to the slow-release prodrug CO-115 ($p < 0.05$). Such findings are similar to those of the CO-103 and CO-104 pairs. Unlike CO-103 or CO-104 with detectable plasma levels after *p.o.* dosage, the plasma levels of CO-115 and CO-116 were both below the quantification limit indicating that the absorption of CO-115 and CO-116 *via* the gastrointestinal system is much lower than that of CO-103 and CO-104. This is likely due to a combination of factors including an increased molecular weight, the presence of a morpholine moiety, and the presence of an extra phenyl group. On the other hand, the higher COHb *AUC* of CO-116 was accompanied with the higher CP-116 plasma level compared to those of CO-115, providing clear evidence that the conversion reaction takes place in the gastrointestinal tract, and the CO absorption into the systemic circulation does not require the absorption of the prodrug itself because of CO’s high diffusion rate and permeability [63].

Because Diels-Alder reaction can be promoted by aqueous medium [6,61,62], CO release and absorption begin at the initial dosing site (the gastrointestinal tract for *p.o.* and the peritoneal cavity for *i.p.*). CO release can occur during the absorption/distribution/elimination process of CO prodrugs. Therefore, the pharmacokinetic properties of CO are the net result of the interplay among the reaction kinetics of a CO prodrug at the administration site and in the systemic circulation, CO diffusion/Hb binding/elimination, as well as the biodisposition of the CO prodrug. Hence, a relationship among different pathways that may impact the overall *in vivo* behavior of CO, CO prodrugs, and CP products was proposed (Fig. 8). This helps explain the difference between the pharmacokinetics of the CO/CP compounds and COHb. For example, although the bioavailability of CO-103 was

markedly higher in *i.p.*-dosed mice compared to *p.o.* administration (Table 2), more sustained COHb elevation was observed in *p.o.*-dosed mice (Fig. 5). More detailed pharmacokinetic parameters of CO-103, CP-103, and CP-125 can be found in Supplementary Table S2. It is reported that the hemoglobin level in mice is around 10–17 g/dl [64], which corresponds to a concentration of 6.2–10.6 mM. Considering a 20 g mouse would have about 1.2 ml of blood (58.5 ml/kg [65]), the total hemoglobin would be 7.4–12.6 μmol. Administration of 5 mg/kg *i.v.* of CO-103 would give 0.24 μmol CO in total, which can theoretically lead to a 1.9–3.2% increase of the COHb level above the baseline if all the CO generated completely binds to hemoglobin. This is in good agreement with our experimental findings. Reports also showed that exogenous CO can stimulate HO-1 expression, which could lead to increased CO production [12,15,66–72]. Although the studies conducted here do not allow for examination of the possible contribution of HO-1 (*e.g.* CO prodrug as HO-1 inducer), given the quick onset of COHb elevation after the administration of CO prodrugs (within 1 h), it is unlikely that the transcriptional regulations of HO-1 were a significant contributing factor. However, this is clearly an aspect that needs to be examined in the future.

3.4. Fecal excretion of CO-103 and CP-103 following oral administration in mice

The limited oral absorption of the CO prodrugs and CP products into the systemic circulation suggests the need to study unchanged CO prodrugs and unabsorbed CP products in the gastrointestinal tract. In doing so, fecal analysis was conducted to determine the amount of CO prodrugs and CP products that may be recovered from fecal samples following *p.o.* administration of CO prodrugs. In particular, we focused on the analysis of CO-103 and CP-103. First, an efficient and rapid fecal sample extraction protocol using a salting-out assisted liquid/liquid extraction method with a high recovery ratio (> 85%) was developed to enable the quantification of CO-103 and CP-103 in feces. Both CO-103 and CP-103 were shown to be stable in fecal samples during the entire analytical process by maintaining the samples on ice. The signals of CO-103 and CP-103 were completely resolved from the noisy background of the fecal extracts (Fig. 9). The linear range for the determination of CO-103 and CP-103 levels in feces was 1–40 μg per aliquot of feces (50–80 mg).

Each individually caged mouse produced roughly 500–1000 mg of fecal pellets when food and water were provided without restriction. Following *p.o.* CO-103 dosing (25 mg/kg), negligible amount of CO-103 was detected, while CP-103 was excreted in feces as early as 4 h (Fig. 9), indicating a relatively quick conversion and rapid transit in the digestive tract. This is in large part determined by the gastrointestinal anatomy and physiology of a mouse [73]. A brief gastrointestinal transit time is expected to pose a physiological limit on the CO delivery efficiency especially for CO prodrugs with slow CO release kinetics. The amount of CP-103 recovered in feces accounted for 6% of the administered dose. When CP-103 was given orally at 25 mg/kg, the fecal elimination of the compound was again most abundant between 4 and 14 h. The total unchanged CP-103 recovered averaged 28% of the administered dose. Such results coupled with the oral bioavailability data (Table 2) suggest metabolic degradation of CP-103 in the gastrointestinal tract being a significant factor. HPLC analysis of fecal samples further revealed possible degradation products of CO-103

and CP-103 in feces (Supplementary Fig. S6). The lower fecal recovery of CP-103 in CO-103-administered mice may also be attributed to the incomplete conversion of CO-103 to CP-103 in the gastrointestinal tract or possibly faster absorption of the prodrug than the CP production. It is also plausible that CO-103 and CP-103 may be degraded by other metabolic pathways such as bacterial metabolism or other non-enzymatic transformation such as Michael addition reaction. Nevertheless, considering CP-103 being the major CO-released product recovered from feces and the low oral bioavailability of CO-103, the fecal analysis results provide strong evidence that CO release can take place in the gastrointestinal tract and the fecal excretion is an important elimination pathway for the degraded CO prodrugs and CP products.

Taken together, oral administration of the CO prodrugs (25 mg/kg) including CO-103, CO-104, CO-125, CO-115, and CO-116 all led to elevated COHb levels in the systemic circulation. Table 4 summarizes the systemic CO exposure (COHb *AUC*) following oral administration of all tested CO prodrugs in relation to their physicochemical properties (CO release half-life, lipophilicity) and the oral absorption of intact CO prodrugs. It reveals that the CO release kinetics is the most critical factor that determines the extent of systemic CO exposure. Oral dosing of prodrugs with CO release $t_{1/2}$ of less than 2 h (CO-103, 116, 125) resulted in significantly higher COHb *AUC* levels ($p < 0.05$) in mice than those with slower release ($t_{1/2} > 5$ h, CO-115, 104). Importantly, systemic COHb elevation can be achieved without notable absorption of intact CO prodrugs (CO-116, 125, 115), providing strong evidence that CO is released inside the gastrointestinal tract and gets absorbed systemically. It is interesting to note that COHb peaked at around 1 h for all these CO prodrugs, irrespective of their release kinetics and lipophilicity. Given CO elimination is a continuous process with a half-life of 20 min in mice [74], these results imply that CO absorption occurs rapidly from the upper gastrointestinal region (such as small intestines) soon after ingestion of CO prodrugs, while the CO release kinetics determines the amount of CO being available for absorption from such a region.

From a drug delivery point-of-view, a major advantage of the organic CO prodrug approach is the tunability of CO release kinetics, which allows for optimization to achieve elevated and sustained COHb levels *in vivo*. Further modulation of the lipophilicity and ionization of CO prodrugs allows for the control of CO prodrug absorption. Another potential advantage of the organic CO prodrug approach resides in the tunability of membrane permeability to increase drug distribution to peripheral tissues. Owing to the highly diffusible nature [63] and strong binding affinity of CO to hemoglobin, inhaled CO is distributed in the body predominantly (> 85%) in the form of COHb with less than 10% CO bound with extravascular proteins such as myoglobin and cytochromes, and only less than 1% is in the free dissolved form that is pharmacologically active [75]. The circulating CO prodrugs may potentially overcome this CO delivery bottleneck and achieve intracellular CO delivery. Collectively, these results demonstrate the proof of concept for oral delivery of CO *via* the organic CO prodrugs as well as the directions for future optimization.

After a comprehensive pharmacokinetic analysis on the CO prodrugs as described above, one might wonder whether the level and duration of CO exposure observed here are therapeutically relevant. This is an important question, especially considering the sometimes

confusing results in the literature and the lack of consensus on the COHb level needed for various pharmacological indications. For example in rodent models, some studies demonstrate that therapeutic effects were observed for inhaled CO gas at 10–18% of COHb and 6–10% for some CO-RMs [2,7], while in other studies [11,15,32,33,76] therapeutic effects were observed with less noticeable or even undetectable elevation on the COHb level (0–4%). It is important to note the different CO delivery forms (*e.g.* inhaled CO *vs.* CO-RMs, delivery routes, and frequency) for all these studies, which are known to make a difference in terms of the pharmacological effects and toxicity [22]. One key aspect to consider is the animal model work using the same kind of organic CO prodrugs examined in this study. Along this line, CO-103 exhibited marked anti-inflammatory efficacy in mouse models of colitis at 15 mg/kg *via i.p.* administration [4]. This is right in the middle of the various doses used in the current pharmacokinetic evaluation. Additionally, one of our previous studies using *i.v.* administration of 4 mg/kg of an organic CO prodrug gave a peak COHb level of 4.5% in mice and showed significant protection against acute liver failure [11]. An esterase-sensitive and pH-controlled CO prodrug exhibited pronounced efficacy at 10 mg/kg in mouse models of systemic inflammation and inflammation-induced liver injury [10]. All such results support the notion that the COHb levels observed in this study are pharmacologically relevant.

4. Conclusions

We have conducted the very first pharmacokinetic studies on organic CO prodrugs that previously demonstrated pharmacological efficacy in mice. We examined five organic CO prodrugs with a range of CO release half-lives for their pharmacokinetic behaviors following *i.v.*, *i.p.* and *p.o.* administration. It was found that all three routes were able to deliver CO to the systemic circulation, as indicated by the elevated COHb levels in blood. The CO delivery efficiency followed the order of *i.v.* > *p.o.* > *i.p.*, underscoring that oral administration is a viable route for CO delivery. We are especially interested in the effect of CO release kinetics on the CO delivery efficiency after oral administration. Those that had CO release half-lives of 0.4–1.6 h (CO-103, 116, 125) yielded significantly higher COHb *AUC* levels than those with the release half-lives above 4 h (CO-115, 104). Such results suggest that the CO prodrugs with rapid CO release kinetics are more efficient in oral delivering CO to mice. Moreover, systemic COHb elevation can be achieved without notable oral absorption of CO prodrugs, suggesting the possibility of delivering effective doses of CO to the systemic circulation while keeping systemic exposure of the CO prodrugs to the minimum. The findings and insights from this pharmacokinetic study are important for the future optimization of organic CO prodrugs, as well as formulation development.

Supplementary Material

Refer to Web version on PubMed Central for supplementary material.

Acknowledgment

The work was partially supported by a grant from the National Institutes of Health (R01DK119202). ZP and LKDLC were partially supported by internal MBD and CDT fellowships, respectively, at GSU. We would like to

thank Dr. Nigel Langley from BASF for providing the Kolliphor® HS 15 sample. BW would like to acknowledge support by the Georgia Research Alliance in the form of a GRA Eminent Scholar Endowment.

References

[1]. Ji X, Wang B, Toward carbon monoxide based therapeutics: carbon monoxide in a pill, Pharm. Pat. Anal 6 (2017) 171–177. [PubMed: 28696157]

[2]. Motterlini R, Otterbein LE, The therapeutic potential of carbon monoxide, Nat. Rev. Drug Discov 9 (2010) 728–743. [PubMed: 20811383]

[3]. Wu L, Wang R, Carbon monoxide: endogenous production, physiological functions, and pharmacological applications, Pharmacol. Rev 57 (2005) 585–630. [PubMed: 16382109]

[4]. Ji X, Zhou C, Ji K, Aghoghovbia R, Pan Z, Chittavong V, Ke B, Wang B, Click and release: a chemical strategy toward developing Gasotransmitter prodrugs by using an intramolecular Diels-Alder reaction, Angew. Chem. Int. Ed. Engl 55 (2016) 15846–15851. [PubMed: 27879021]

[5]. Ji X, Damera K, Zheng Y, Yu B, Otterbein LE, Wang B, Toward carbon monoxide-based therapeutics: critical drug delivery and developability issues, J. Pharm. Sci 105 (2016) 406–416 (and references cited therein). [PubMed: 26869408]

[6]. Ji X, Wang B, Strategies toward organic carbon monoxide prodrugs, Acc. Chem. Res 51 (2018) 1377–1385. [PubMed: 29762011]

[7]. Yang X, de Caestecker M, Otterbein LE, Wang B, Carbon monoxide: an emerging therapy for acute kidney injury, Med. Res. Rev 40 (2019) 1147–1177. [PubMed: 31820474]

[8]. Popova M, Soboleva T, Ayad S, Benninghoff AD, Berreau LM, Visible-light-activated quinolone carbon-monoxide-releasing molecule: prodrug and albumin-assisted delivery enables anticancer and potent anti-inflammatory effects, J. Am. Chem. Soc 140 (2018) 9721–9729. [PubMed: 29983046]

[9]. Soboleva T, Berreau LM, Tracking CO release in cells via the luminescence of donor molecules and/or their by-products, Isr. J. Chem 59 (2019) 339–350. [PubMed: 31516159]

[10]. Ji X, Pan Z, Li C, Kang T, De La Cruz LKC, Yang L, Yuan Z, Ke B, Wang B, Esterase-sensitive and pH-controlled carbon monoxide prodrugs for treating systemic inflammation, J. Med. Chem 62 (2019) 3163–3168. [PubMed: 30816714]

[11]. Zheng Y, Ji X, Yu B, Ji K, Gallo D, Csizmadia E, Zhu M, de la Cruz LKC, Choudhary MR, Chittavong V, Pan Z, Yuan Z, Otterbein LE, Wang B, Enrichment-triggered prodrug activation demonstrated through mitochondria-targeted delivery of doxorubicin and carbon monoxide, Nat. Chem 10 (2018) 787–794. [PubMed: 29760413]

[12]. Upadhyay KK, Jadeja RN, Thadani JM, Joshi A, Vohra A, Mevada V, Patel R, Khurana S, Devkar RV, Carbon monoxide releasing molecule A-1 attenuates acetaminophen-mediated hepatotoxicity and improves survival of mice by induction of Nrf2 and related genes, Toxicol. Appl. Pharmacol 360 (2018) 99–108. [PubMed: 30273691]

[13]. Correa-Costa M, Gallo D, Csizmadia E, Gomperts E, Lieberum JL, Hauser CJ, Ji X, Wang B, Camara NOS, Robson SC, Otterbein LE, Carbon monoxide protects the kidney through the central circadian clock and CD39, Proc. Natl. Acad. Sci. U. S. A 115 (2018) E2302–E2310. [PubMed: 29463714]

[14]. Fredenburgh LE, Perrella MA, Barragan-Bradford D, Hess DR, Peters E, Welty-Wolf KE, Kraft BD, Harris RS, Maurer R, Nakahira K, Oromendia C, Davies JD, Higuera A, Schiffer KT, Englert JA, Dieffenbach PB, Berlin DA, Lagambina S, Bouthot M, Sullivan AI, Nuccio PF, Kone MT, Malik MJ, Porras MAP, Finkelsztein E, Winkler T, Hurwitz S, Serhan CN, Piantadosi CA, Baron RM, Thompson BT, Choi AM, A phase I trial of low-dose inhaled carbon monoxide in sepsis-induced ARDS, JCI Insight 3 (2018).

[15]. Belcher JD, Gomperts E, Nguyen J, Chen C, Abdulla F, Kiser ZM, Gallo D, Levy H, Otterbein LE, Vercellotti GM, Oral carbon monoxide therapy in murine sickle cell disease: beneficial effects on vaso-occlusion, inflammation and anemia, PLoS ONE 13 (2018) e0205194. [PubMed: 30308028]

[16]. Faizan M, Muhammad N, Niazi KUK, Hu Y, Wang Y, Wu Y, Sun H, Liu R, Dong W, Zhang W, Gao Z, CO-releasing materials: an emphasis on therapeutic implications, as release and subsequent cytotoxicity are the part of therapy, Materials (Basel) 12 (2019) 1643.

[17]. Soboleva T, Esquer HJ, Anderson SN, Berreau LM, Benninghoff AD, Mitochondrial-localized versus cytosolic intracellular CO-releasing organic PhotoCORMs: evaluation of CO effects using bioenergetics, ACS Chem. Biol 13 (2018) 2220–2228. [PubMed: 29932318]

[18]. Poloukhtine A, Popik VV, Mechanism of the cyclopropenone decarbonylation reaction. A density functional theory and transient spectroscopy study, J. Phys. Chem. A 110 (2006) 1749–1757. [PubMed: 16451004]

[19]. Peng P, Wang C, Shi Z, Johns VK, Ma L, Oyer J, Copik A, Igarashi R, Liao Y, Visible-light activatable organic CO-releasing molecules (PhotoCORMs) that simultaneously generate fluorophores, Org. Biomol. Chem. 11 (2013) 6671–6674. [PubMed: 23943038]

[20]. Palao E, Slanina T, Muchova L, Solomek T, Vitek L, Klan P, Transition-metal-free CO-releasing BODIPY derivatives activatable by visible to NIR light as promising bioactive molecules, J. Am. Chem. Soc 138 (2016) 126–133. [PubMed: 26697725]

[21]. Abeyrathna N, Washington K, Bashur C, Liao Y, Nonmetallic carbon monoxide releasing molecules (CORMs), Org. Biomol. Chem 15 (2017) 8692–8699. [PubMed: 28948260]

[22]. Yang X, Ke B, Lu W, Wang B, CO as a therapeutic agent: discovery and delivery forms, Chin. J. Nat. Med 18 (2020) 284–295. [PubMed: 32402406]

[23]. McKendrick JG, Snodgrass W, On the physiological action of carbon monoxide of nickel, Br. Med. J 1 (1891) 1215–1217.

[24]. Motterlini R, Foresti R, Green CJ, Chapter 6. Studies on the development of carbon monoxide-releasing molecules: potential applications for the treatment of cardiovascular dysfunction, in: Wang R (Ed.), Carbon Monoxide and Cardiovascular Functions, Routledge, 2002, pp. 249–271.

[25]. Mann B, CO-releasing molecules: a personal view, Organometallics 31 (2012) 5728–5735 (and references cited therein).

[26]. McLean S, Mann BE, Poole RK, Sulfite species enhance carbon monoxide release from CO-releasing molecules: implications for the deoxymyoglobin assay of activity, Anal. Biochem 427 (2012) 36–40. [PubMed: 22561917]

[27]. Santos-Silva T, Mukhopadhyay A, Seixas JD, Bernardes GJ, Romao CC, Romao MJ, Towards improved therapeutic CORMs: understanding the reactivity of CORM-3 with proteins, Curr. Med. Chem 18 (2011) 3361–3366. [PubMed: 21728965]

[28]. Santos-Silva T, Mukhopadhyay A, Seixas JD, Bernardes GJ, Romao CC, Romao MJ, CORM-3 reactivity toward proteins: the crystal structure of a Ru(II) dicarbonyl-lysozyme complex, J. Am. Chem. Soc 133 (2011) 1192–1195. [PubMed: 21204537]

[29]. Ling K, Men F, Wang WC, Zhou YQ, Zhang HW, Ye DW, Carbon monoxide and its controlled release: therapeutic application, detection, and development of carbon monoxide releasing molecules (CORMs), J. Med. Chem 61 (2018) 2611–2635. [PubMed: 28876065]

[30]. Romanski S, Stamellou E, Jaraba JT, Storz D, Kramer BK, Hafner M, Amslinger S, Schmalz HG, Yard BA, Enzyme-triggered CO-releasing molecules (ET-CORMs): evaluation of biological activity in relation to their structure, Free Radic. Biol. Med 65 (2013) 78–88. [PubMed: 23774042]

[31]. Pierri AE, Huang PJ, Garcia JV, Stanfill JG, Chui M, Wu G, Zheng N, Ford PC, A photoCORM nanocarrier for CO release using NIR light, Chem. Commun 51 (2015) 2072–2075.

[32]. Steiger C, Uchiyama K, Takagi T, Mizushima K, Higashimura Y, Gutmann M, Hermann C, Botov S, Schmalz HG, Naito Y, Meinel L, Prevention of colitis by controlled oral drug delivery of carbon monoxide, J. Control. Release 239 (2016) 128–136. [PubMed: 27578097]

[33]. Yin H, Fang J, Liao L, Nakamura H, Maeda H, Styrene-maleic acid copolymer-encapsulated CORM2, a water-soluble carbon monoxide (CO) donor with a constant CO-releasing property, exhibits therapeutic potential for inflammatory bowel disease, J. Control. Release 187 (2014) 14–21. [PubMed: 24852097]

[34]. Motterlini R, Nikam A, Manin S, Ollivier A, Wilson JL, Djouadi S, Muchova L, Martens T, Rivard M, Foresti R, HYCO-3, a dual CO-releaser/Nrf2 activator, reduces tissue inflammation in mice challenged with lipopolysaccharide, Redox Biol. 20 (2019) 334–348. [PubMed: 30391826]

[35]. Ollivier A, Foresti R, El Ali Z, Martens T, Kitagishi H, Motterlini R, Rivard M, Design and biological evaluation of Manganese- and Ruthenium-based hybrid CO-RMs (HYCOs), ChemMedChem 14 (2019) 1684–1691. [PubMed: 31319021]

[36]. Southam HM, Smith TW, Lyon RL, Liao C, Trevitt CR, Middlemiss LA, Cox FL, Chapman JA, El-Khamisy SF, Hippler M, Williamson MP, Henderson PJF, Poole RK, A thiol-reactive Ru(II) ion, not CO release, underlies the potent antimicrobial and cytotoxic properties of CO-releasing molecule-3, Redox Biol. 18 (2018) 114–123. [PubMed: 30007887]

[37]. Winburn IC, Gunatunga K, McKernan RD, Walker RJ, Sammut IA, Harrison JC, Cell damage following carbon monoxide releasing molecule exposure: implications for therapeutic applications, Basic Clin. Pharmacol. Toxicol 111 (2012) 31–41. [PubMed: 22269084]

[38]. Stucki D, Krahl H, Walter M, Steinhausen J, Hommel K, Brenneisen P, Stahl W, Effects of frequently applied carbon monoxide releasing molecules (CORMs) in typical CO-sensitive model systems a comparative in vitro study, Arch. Biochem. Biophys 687 (2020) 108383. [PubMed: 32335048]

[39]. Nielsen VG, Garza JI, Comparison of the effects of CORM-2, CORM-3 and CORM-A1 on coagulation in human plasma, Blood Coagul. Fibrinolysis 25 (2014) 801–805. [PubMed: 25058038]

[40]. Nielsen VG, The anticoagulant effect of Apis mellifera phospholipase A2 is inhibited by CORM-2 via a carbon monoxide-independent mechanism, J. Thromb. Thrombolysis 49 (2019) 100–107.

[41]. Yuan Z, Yang X, De la Cruz L, Wang B, et al., Nitro reduction-based fluorescent probes for carbon monoxide require reactivity involving a ruthenium carbonyl moiety, Chem. Commun 56 (2020) 2190–2193.

[42]. Sutton DA, Popik VV, Sequential photochemistry of dibenzo[a,e]dicyclopropa [c,g] [8]annulene-1,6-dione: selective formation of didehydrodibenzo[a,e][8]annulenes with ultrafast SPAAC reactivity, J. Org. Chem 81 (2016) 8850–8857. [PubMed: 27635662]

[43]. Vandegriff KD, Young MA, Lohman J, Bellelli A, Samaja M, Malavalli A, Winslow RM, CO-MP4, a polyethylene glycol-conjugated haemoglobin derivative and carbon monoxide carrier that reduces myocardial infarct size in rats, Br. J. Pharmacol 154 (2008) 1649–1661. [PubMed: 18536756]

[44]. Sakai H, Horinouchi H, Tsuchida E, Kobayashi K, Hemoglobin vesicles and red blood cells as carriers of carbon monoxide prior to oxygen for resuscitation after hemorrhagic shock in a rat model, Shock 31 (2009) 507–514. [PubMed: 18827742]

[45]. Pinto MN, Chakraborty I, Sandoval C, Mascharak PK, Eradication of HT-29 colorectal adenocarcinoma cells by controlled photorelease of CO from a CO-releasing polymer (photoCORP-1) triggered by visible light through an optical fiber-based device, J. Control. Release 264 (2017) 192–202. [PubMed: 28866022]

[46]. Wang D, Viennois E, Ji K, Damera K, Draganov A, Zheng Y, Dai C, Merlin D, Wang B, A click-and-release approach to CO prodrugs, Chem. Commun 50 (2014) 15890–15893.

[47]. Ji X, de La Cruz LK, Pan Z, Chittavong V, Wang B, pH-sensitive metal-free carbon monoxide prodrugs with tunable and predictable release rates, Chem. Commun 53 (2017) 9628–9631.

[48]. Ji X, Ji K, Chittavong V, Yu B, Pan Z, Wang B, An esterase-activated click and release approach to metal-free CO-prodrugs, Chem. Commun 53 (2017) 8296–8299.

[49]. Xie J, Zhang X, Xu J, Zhang Z, Klingensmith NJ, Liu S, Pan C, Yang Y, Qiu H, Effect of remote ischemic preconditioning on outcomes in adult cardiac surgery: a systematic review and meta-analysis of randomized controlled studies, Anesth. Analg 127 (2018) 30–38. [PubMed: 29210794]

[50]. De La Cruz K, Benoit SL, Pan Z, Maier R, Ji X, Wang B, Click, release, and fluoresce: a chemical strategy for a cascade prodrug system for codelivery of carbon monoxide, a drug payload, and a fluorescent reporter, Org. Lett 20 (2018) 897–900. [PubMed: 29380605]

[51]. Ji X, Ji K, Chittavong V, Aghoghovbia RE, Zhu M, Wang B, Click and fluoresce: a bioorthogonally activated smart probe for wash-free fluorescent labeling of bio-molecules, J. Org. Chem 82 (2017) 1471–1476. [PubMed: 28067514]

[52]. Ji X, Aghoghovbia RE, De La Cruz LKC, Pan Z, Yang X, Yu B, Wang B, Click and release: a high-content bioorthogonal prodrug with multiple outputs, Org. Lett 21 (2019) 3649–3652. [PubMed: 31063383]

[53]. Kueh JTB, Stanley NJ, Hewitt RJ, Woods LM, Larsen L, Harrison JC, Rennison D, Brimble MA, Sammut IA, Larsen DS, Norborn-2-en-7-ones as physiologically-triggered carbon monoxide-releasing prodrugs, Chem. Sci 8 (2017) 5454–5459. [PubMed: 28970925]

[54]. Pan Z, Ji X, Chittavong V, Li W, Ji K, Zhu M, Zhang J, Wang B, Organic CO-prodrugs: structure CO-release rate relationship studies, Chem. Eur. J 23 (2017) 9838–9845. [PubMed: 28544290]

[55]. Bakalarz D, Surmiak M, Yang X, Wójcik D, Korbut E, Śliwowski Z, Ginter G, Buszewicz G, Brzozowski T, Cieszkowski J, Głowacka U, Magierowska K, Pan Z, Wang B, Magierowski M, Organic carbon monoxide prodrug, BW-CO-111 in protection against chemically-induced gastric mucosal damage, Acta Pharm. Sin. B 10 (2020) In press.

[56]. Yoshida M, Akane A, Nishikawa M, Watabiki T, Tsuchihashi H, Extraction of thiamylal in serum using hydrophilic acetonitrile with subzero-temperature and salting-out methods, Anal. Chem. 76 (2004) 4672–4675. [PubMed: 15307775]

[57]. Zhang J, Wu H, Kim E, El-Shourbagy TA, Salting-out assisted liquid/liquid extraction with acetonitrile: a new high throughput sample preparation technique for good laboratory practice bioanalysis using liquid chromatography-mass spectrometry, Biomed. Chromatogr 23 (2009) 419–425. [PubMed: 19016229]

[58]. Wu H, Zhang J, Norem K, El-Shourbagy TA, Simultaneous determination of a hydrophobic drug candidate and its metabolite in human plasma with salting-out assisted liquid/liquid extraction using a mass spectrometry friendly salt, J. Pharm. Biomed. Anal 48 (2008) 1243–1248. [PubMed: 18926659]

[59]. Kamath AV, Wang J, Lee FY, Marathe PH, Preclinical pharmacokinetics and in vitro metabolism of dasatinib (BMS-354825): a potent oral multi-targeted kinase inhibitor against SRC and BCR-ABL, Cancer Chemother. Pharmacol 61 (2008) 365–376. [PubMed: 17429625]

[60]. Lee KJ, Mower R, Hollenbeck T, Castelo J, Johnson N, Gordon P, Sinko PJ, Holme K, Lee YH, Modulation of nonspecific binding in ultrafiltration protein binding studies, Pharm. Res 20 (2003) 1015–1021. [PubMed: 12880287]

[61]. Rideout DC, Breslow R, Hydrophobic acceleration of Diels-Alder reactions, J. Am. Chem. Soc 102 (1980) 7816–7817.

[62]. Blokzijl W, Blandamer MJ, Engberts JBFN, Diels-Alder reactions in aqueous solutions. Enforced hydrophobic interactions between diene and dienophile, J. Am. Chem. Soc 113 (1991) 4241–4246.

[63]. Sakurai Y, The study on the skin permeability of carbon monoxide and measurement of carboxy-hemoglobin in blood, Jap. J. Legal Med 17 (1963) 314–326.

[64]. Fox JG, Barthold S, Davisson M, Newcomer CE, Quimby FW, Smith A, The Mouse in Biomedical Research: Normative Biology, Husbandry, and Models, Elsevier Science, 2006.

[65]. Tian X, Nyberg S, Sharp PS, Madsen J, Daneshpour N, Armes SP, Berwick J, Azzouz M, Shaw P, Abbott NJ, Battaglia G, LRP-1-mediated intracellular anti-body delivery to the central nervous system, Sci. Rep 5 (2015) 11990. [PubMed: 26189707]

[66]. Lin CC, Yang CC, Hsiao LD, Chen SY, Yang CM, Heme oxygenase-1 induction by carbon monoxide releasing molecule-3 suppresses interleukin-1beta-mediated neuroinflammation, Front. Mol. Neurosci 10 (2017) 387. [PubMed: 29209167]

[67]. Chi PL, Lin CC, Chen YW, Hsiao LD, Yang CM, CO induces Nrf2-dependent heme oxygenase-1 transcription by cooperating with Sp1 and c-Jun in rat brain astrocytes, Mol. Neurobiol 52 (2015) 277–292. [PubMed: 25148934]

[68]. Lin CC, Hsiao LD, Cho RL, Yang CM, CO-releasing molecule-2 induces Nrf2/ARE-dependent heme oxygenase-1 expression suppressing TNF-α-induced pulmonary inflammation, J. Clin. Med 8 (2019) 436.

[69]. Lin CC, Hsiao LD, Cho RL, Yang CM, Carbon monoxide releasing molecule-2-upregulated ROS-dependent heme oxygenase-1 axis suppresses lipopolysaccharide-induced airway inflammation, Int. J. Mol. Sci 20 (2019) 3157.

[70]. Wysokinski D, Lewandowska P, Zatak D, Juszczak M, Kluska M, Lizinska D, Rudolf B, Wozniak K, Photoactive CO-releasing complexes containing iron genotoxicity and ability in HO-1 gene induction in HL-60 cells, Toxicol. Res 8 (2019) 544–551.

[71]. Upadhyay KK, Jadeja RN, Vyas HS, Pandya B, Joshi A, Vohra A, Thounaojam MC, Martin PM, Bartoli M, Devkar RV, Carbon monoxide releasing molecule-A1 improves nonalcoholic steatohepatitis via Nrf2 activation mediated improvement in oxidative stress and mitochondrial function, Redox Biol. 28 (2020) 101314. [PubMed: 31514051]

[72]. Zhou L, Ao L, Yan Y, Li C, Li W, Ye A, Liu J, Hu Y, Fang W, Li Y, Levocorydalmine attenuates vincristine-induced neuropathic pain in mice by upregulating the Nrf2/HO-1/CO pathway to inhibit connexin 43 expression, Neurotherapeutics 17 (2020) 340–355. [PubMed: 31617070]

[73]. Padmanabhan P, Grosse J, Asad AB, Radda GK, Golay X, Gastrointestinal transit measurements in mice with 99mTc-DTPA-labeled activated charcoal using NanoSPECT-CT, EJNMMI Res. 3 (2013) 60. [PubMed: 23915679]

[74]. Hardy KR, Thom SR, Pathophysiology and treatment of carbon monoxide poisoning, J. Toxicol. Clin. Toxicol 32 (1994) 613–629. [PubMed: 7966524]

[75]. Tyuma I, Ueda Y, Imaizumi K, Kosaka H, Prediction of the carbonmonoxyhemoglobin levels during and after carbon monoxide exposures in various animal species, Jpn. J. Physiol 31 (1981) 131–143. [PubMed: 7289220]

[76]. Pena AC, Penacho N, Mancio-Silva L, Neres R, Seixas JD, Fernandes AC, Romao CC, Mota MM, Bernardes GJ, Pamplona A, A novel carbon monoxide-releasing molecule fully protects mice from severe malaria, Antimicrob. Agents Chemother 56 (2012) 1281–1290. [PubMed: 22155828]

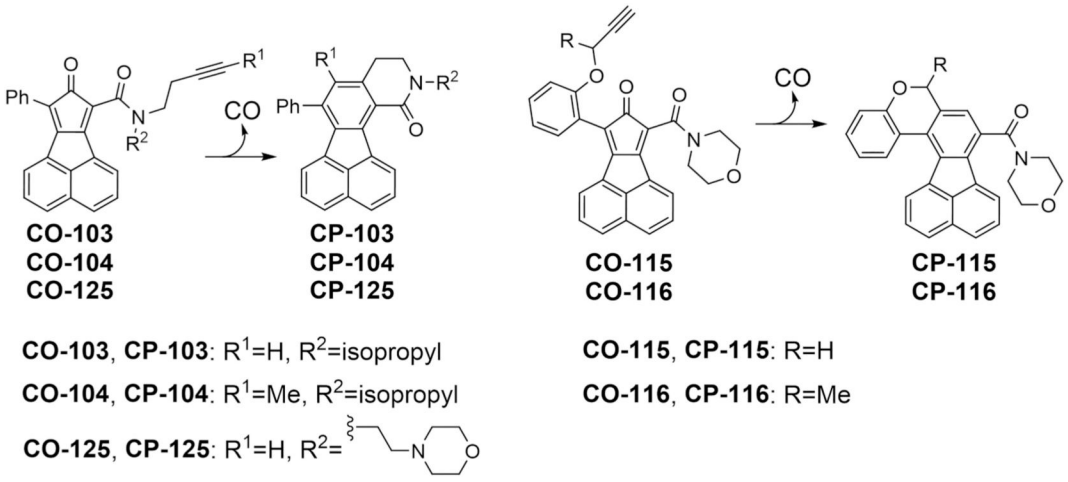

Fig. 1.

The chemical structures of the CO prodrugs and the corresponding CP products after CO release.

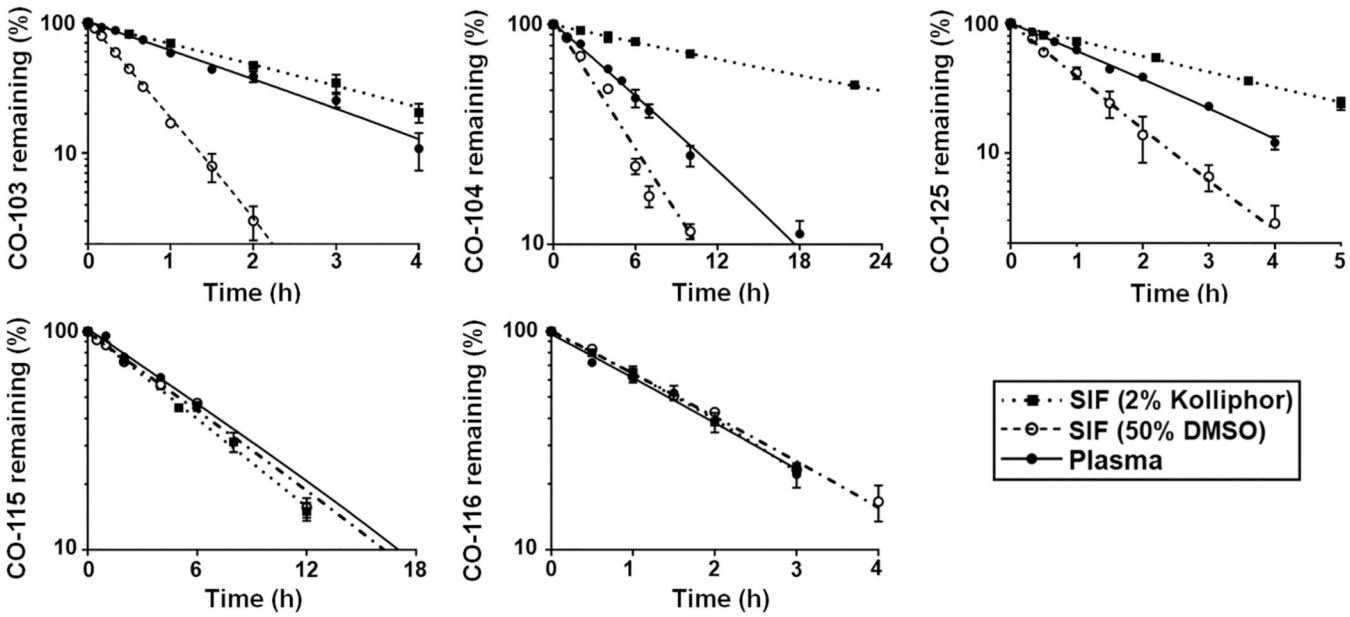

Fig. 2.

Reaction kinetics of CO prodrugs in SIF (50% DMSO), SIF (2% Kolliphor) and plasma at 37 °C as a function of incubation time. The lines represent the respective best-fit regression for each data set. Results are presented as the mean ± SD ($n \geq 3$).

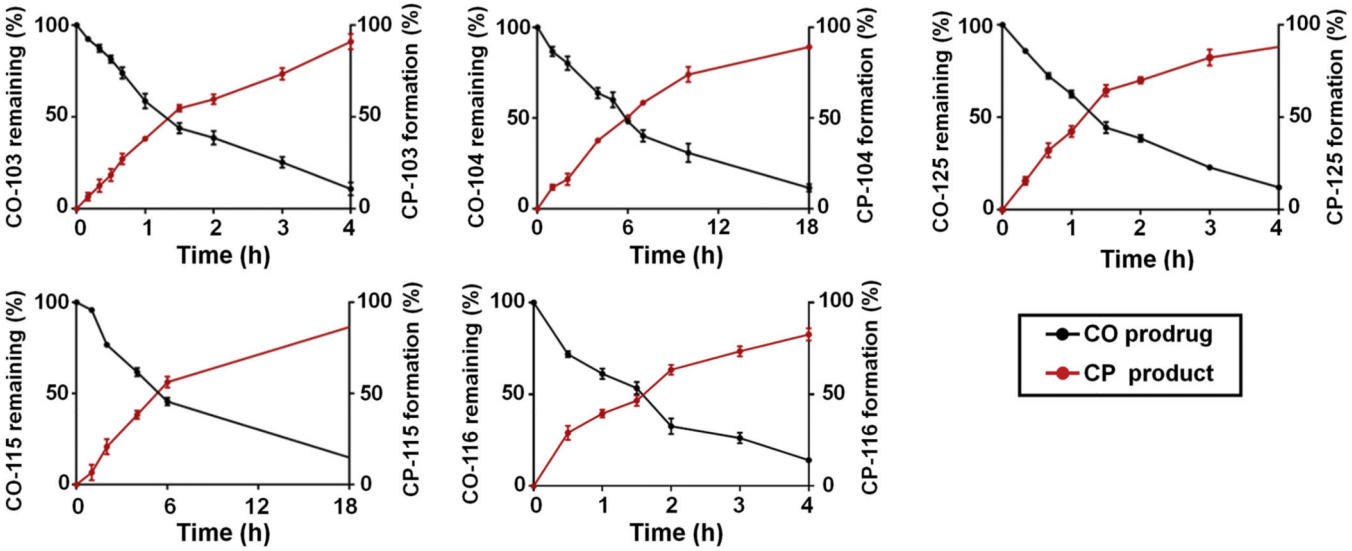

Fig. 3.

Stoichiometric transformation of CO prodrugs to CP prodrugs in plasma at 37 °C. Results are presented as the mean ± SD ($n \geq 3$).

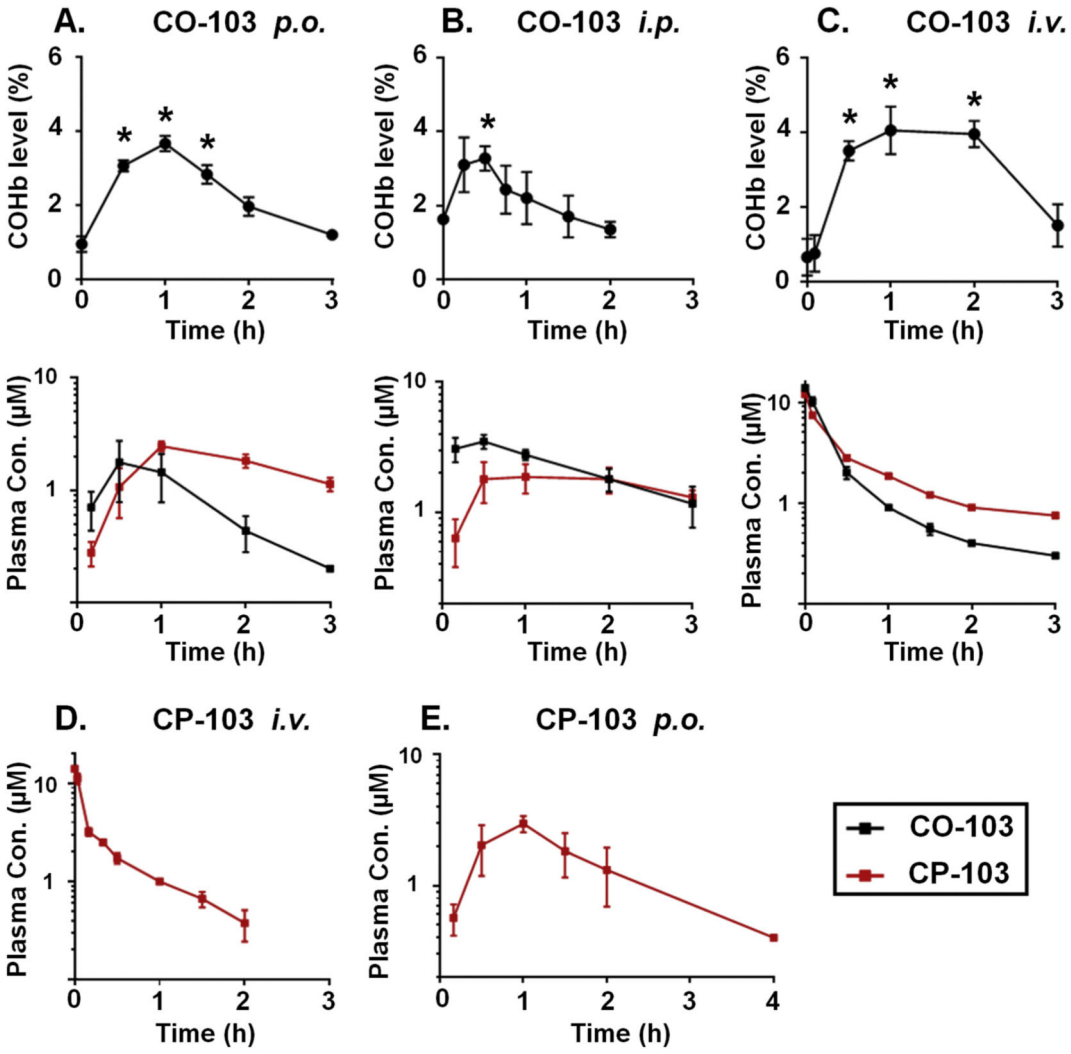

Fig. 4.

Pharmacokinetics of CO-103 and CP-103 in mice. COHb level in blood, CO-103 and CP-103 plasma levels following (A) *p.o.* administration of CO-103 (25 mg/kg); (B) *i.p.* administration of CO-103 (25 mg/kg); and (C) *i.v.* administration of CO-103 (5 mg/kg); CP-103 plasma level following (D) *i.v.* administration of pure CP-103 (5 mg/kg) and (E) *p.o.* administration of pure CP-103 (25 mg/kg). Results are presented as the mean ± SD ($n \geq 3$). * denotes $p < 0.05$ above the baseline.

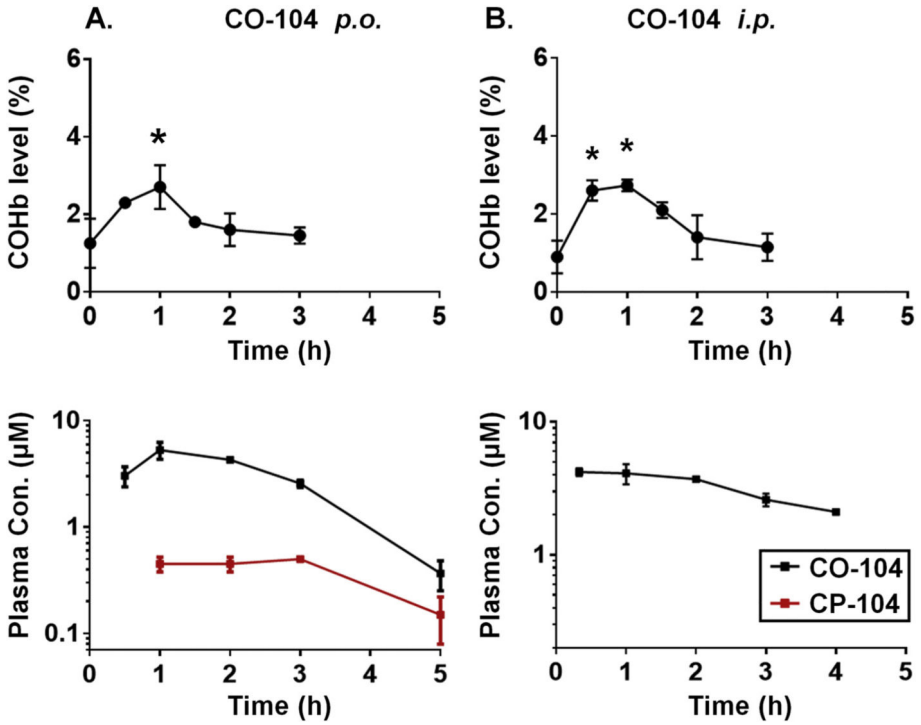

Fig. 5.

Pharmacokinetics of CO-104 in mice. The *COHb* level, CO-104 and CP-104 plasma levels following (A) *p.o.* administration of CO-104 (25 mg/kg); (B) *i.p.* administration of CO-104 (25 mg/kg). Results are presented as the mean ± SD ($n \geq 3$). * denotes $p < 0.05$ above the baseline.

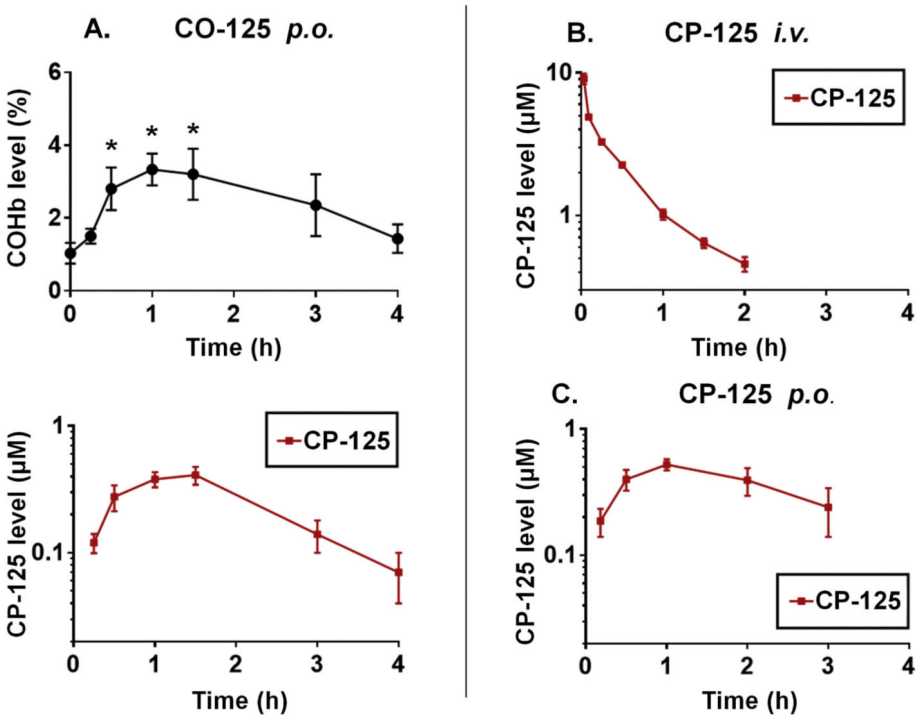

Fig. 6.

Pharmacokinetics of CO-125 and CP-125 in mice. (A) *COHb* level and plasma levels of CO-125 and CP-125 following *p.o.* administration of CO-125 (25 mg/kg); Plasma level of CP-125 following: (B) *i.v.* administration of pure CP-125 (3 mg/kg); (C) *p.o.* administration of pure CP-125 (15 mg/kg). Results are presented as the mean ± SD ($n \geq 3$). * denotes $p < 0.05$ above the baseline.

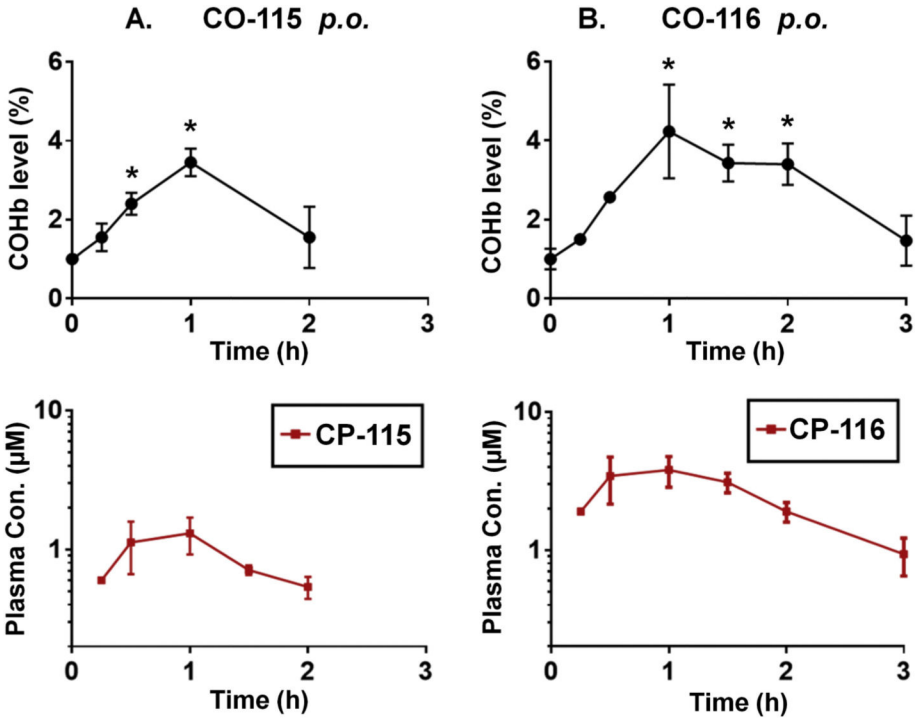

Fig. 7.

Pharmacokinetics of CO-115 and CO-116. *COHb* level and CP product plasma levels were quantified following *p.o.* administration of CO-115 (A) and CO-116 (B) at 25 mg/kg. Results are presented as the mean ± SD (n ≥ 3).* denotes $p < 0.05$ above the baseline.

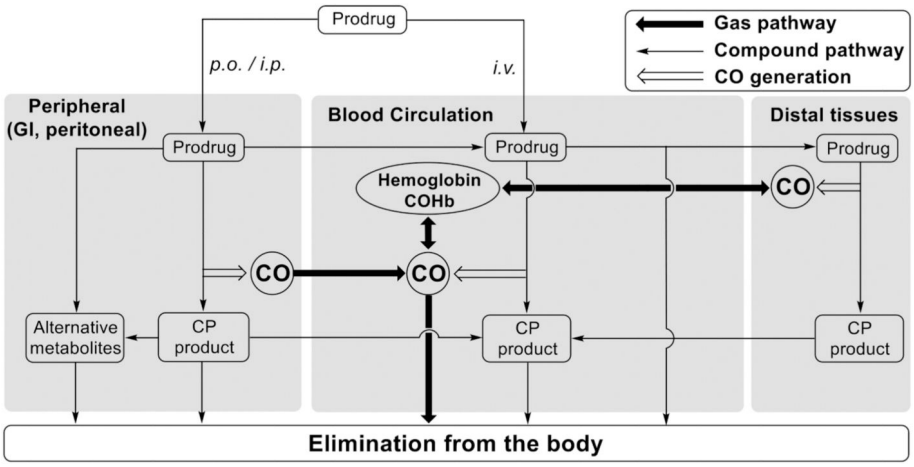

Fig. 8.

Various factors that impact the pharmacokinetic behaviors of CO prodrugs/CP products and CO.

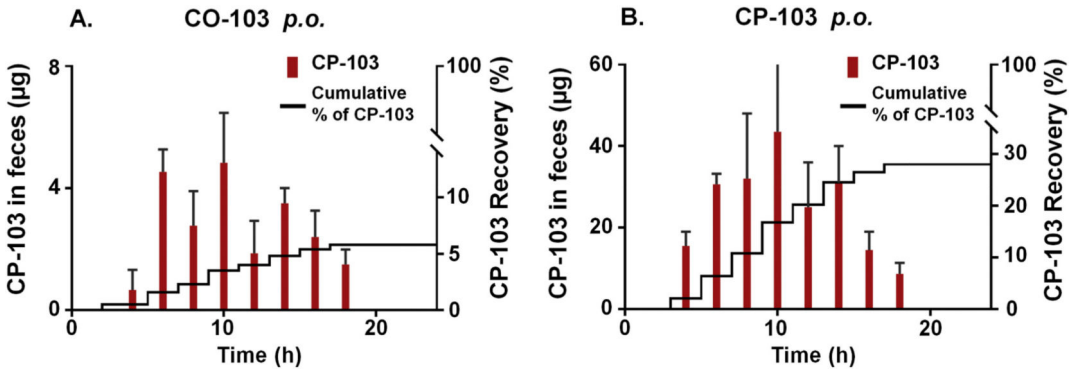

Fig. 9.

CP-103 recovered in feces following *p.o.* administration of (A) CO-103 and (B) pure CP-103 at 25 mg/kg in mice. The right y-axis shows the cumulative percentage of CP-103 recovery over time. Results are presented as the mean ± SD ($n \geq 3$).

Table 1

Reaction kinetics of the CO prodrugs in various media.

Compound	Media	Plasma binding (%)	k (h^{-1})	$t_{1/2}$(h)	r^2
CO-103	SIF (2% Kolliphor)		0.357 ± 0.036	1.93 ± 0.18	0.989
	SIF (50% DMSO)		1.644 ± 0.027	0.42 ± 0.01	0.998
	Plasma	92 ± 1	0.541 ± 0.05	1.29 ± 0.12	0.99
CO-104	SIF (2% Kolliphor)		0.036 ± 0.006	17.56 ± 0.82	0.991
	SIF (50% DMSO)		0.165 ± 0.013	4.22 ± 0.33	0.984
	Plasma	91 ± 1	0.116 ± 0.002	5.99 ± 0.11	0.997
CO-125	SIF (2% Kolliphor)		0.297 ± 0.041	2.33 ± 0.21	0.991
	SIF (50% DMSO)		0.926 ± 0.038	0.75 ± 0.03	0.986
	Plasma	90 ± 2	0.476 ± 0.016	1.55 ± 0.05	0.995
CO-115	SIF (2% Kolliphor)		0.152 ± 0.013	4.85 ± 0.35	0.997
	SIF (50% DMSO)		0.109 ± 0.008	6.39 ± 0.46	0.993
	Plasma	84 ± 1	0.136 ± 0.007	5.11 ± 0.26	0.988
CO-116	SIF (2% Kolliphor)		0.401 ± 0.075	1.82 ± 0.15	0.997
	SIF (50% DMSO)		0.384 ± 0.025	1.58 ± 0.12	0.994
	Plasma	84 ± 2	0.473 ± 0.051	1.48 ± 0.16	0.978

k: first-order rate constant for the conversion reactions of prodrugs; $t_{1/2}$: conversion half-life for the conversion reactions of prodrugs; r^2: measure of the goodness of fit for the nonlinear regression; Results are presented as the mean ± SD ($n \geq 3$).

Table 2

Pharmacokinetic parameters of **CO-103** and **CP-103**.

Compound	Route	Dose (mg/kg)	$t_{1/2}$(h)	$AUC_{0-\infty}$(μM h)	F (%)	COHb AUC (%·h)	CO delivery efficiency (%)
CO-103	*i.v.*	5	1.1 ± 0.3	5.2 ± 0.5	100	7.0 ± 0.9	100
	p.o.	25	0.7 ± 0.1	2.4 ± 0.7	9.2	4.1 ± 0.3	11.7
	i.p.	25	1.5 ± 0.4	8.8 ± 2.4	33.8	1.3 ± 0.3	3.7
CP-103 (from CO-103)	*i.v.*	5	1.7 ± 0.2	8.0 ± 0.4			
	p.o.	25	1.8 ± 0.3	7.7 ± 0.6			
	i.p.	25	2.9 ± 0.4	10.3 ± 1.1			
CP-103 (pure)	*i.v.*	5	0.7 ± 0.2	3.9 ± 0.2	100		
	p.o.	25	1.1 ± 0.2	5.7 ± 1.4	29.2		

t1/2: terminal half-life; *AUC0 – ∞*: area under the plasma drug concentration curve from time zero to infinity; *F*: bioavailability; COHb *AUC*: area under the curve for blood *COHb* level subtracting the pre-administration baseline from time zero to the last sampling time point; CO delivery efficiency: the percentage of COHb *AUC* in relation to that of *i.v.* dosing. Results are presented as the mean ± SD ($n \geq 3$).

Table 3

Pharmacokinetic parameters of **CP-125**.

Compound	Route	Dose (mg/kg)	$t_{1/2}$(h)	$AUC_{0-\infty}$(μM h)	F (%)
CP-125 (pure)	*i.v.*	3	0.9 ± 0.1	4.1 ± 0.3	100
	p.o.	15	1.4 ± 0.2	1.3 ± 0.4	6.3
CP-125 (from CO-125)	*p.o.*	25	1.0 ± 0.1	1.1 ± 0.3	

$t_{1/2}$: terminal half-life; $AUC_{0-\infty}$: area under the plasma drug concentration curve from time zero to infinity; *F*: bioavailability. Results are presented as the mean ± SD (n ≥ 3).

Table 4

In vivo CO exposure versus physicochemical properties of prodrugs.

Compound	$t_{1/2}$(h)	COHb AUC (%·h)	Oral absorption of intact CO prodrugs	Ranking of lipophilicity (1 being strongest)
CO-103	0.4	4.1 ± 0.3	Yes	2
CO-125	0.8	6.1 ± 1.4	No	3
CO-116	1.6	5.6 ± 1.1	No	4
CO-104	4.2	2.3 ± 0.4	Yes	1
CO-115	6.4	2.2 ± 0.5	No	5

$t_{1/2}$: release half-life of CO prodrug in SIF (50% DMSO); COHb *AUC*: area under the curve for blood COHb level subtracting the pre-administration baseline from time zero to the last sampling time point. Results are presented as the mean ± SD (n ≥ 3).